Articles

^{13}C NMR Analysis of α-Olefin Enchainment in Poly(α-olefins) Produced with Nickel and Palladium α-Diimine Catalysts

Elizabeth F. McCord,* Stephan J. McLain, Lissa T. J. Nelson, and Steven D. Ittel*

DuPont Central Research,† Experimental Station, Wilmington, Delaware 19880-0328

Daniel Tempel, Christopher M. Killian, Lynda K. Johnson, and Maurice Brookhart*

Department of Chemistry, University of North Carolina, Chapel Hill, North Carolina 27599-3290

Received July 10, 2006; Revised Manuscript Received October 5, 2006

ABSTRACT: α-Diimine complexes of palladium and nickel catalyze the polymerization of α-olefins to give new materials that range from low-T_g elastomers to low-melting, partially crystalline polymers. The ^{1}H and ^{13}C NMR spectra of the resulting polymers have been assigned in detail. Many unique microstructural features of the complex polymers have been identified. Mechanistic models that involve the 1,2- and 2,1-insertion of the α-olefins, chain walking, and insertion at certain points along the chain have been constructed. The complex microstructures can be explained using a small set of rules for palladium catalysts which is expanded slightly to account for the nickel catalysts.

Introduction

Prior to the discovery of α-diimine catalysts, reports of polymerization of α-olefins by late metal catalysts were rare. A nickel aminobis(imino)phosphorane catalyst has been reported to oligomerize α-olefins with exclusively 2,ω-enchainment.[1,2] The mechanism proposed for this polymerization involves 1,2-insertion followed by chain-walking of the Ni to the end of the chain prior to the next insertion. Palladium cyanide has been reported to polymerize propene in a 1,3-fashion to give a crystalline polymer equivalent to a 93:7 ethylene:propene copolymer.[3]

A new class of polymerization catalysts based on aryl-substituted α-diimine complexes of Ni and Pd was reported in 1995 by Johnson, Killian, and Brookhart.[4] These catalysts are capable of polymerizing both ethylene and α-olefins. This and subsequent related work[5,6] have been the subjects of several reviews.[7−9] Polymers prepared using these catalysts have unique microstructures that can be accounted for by simple mechanistic models. Previous papers have described the structures of the resulting polyethylenes[10] and polypropylenes,[11] mechanistic aspects of their formation,[12−14] and living polymerizations of α-olefins.[15]

We have reported a detailed analysis of the enchainment of propylene in polypropylene made with Ni and Pd diimine catalysts which clearly established that 1,2- and 1,3-enchainment are competitive processes.[11] 1,3-Enchainment results from 2,1-insertion followed by chain-walking. For certain Ni diimine catalysts there are a large number of 2,1-insertions and adjacent 1,3-enchainments.

Since our initial reports several related studies have appeared from other groups. Pellecchia showed that the regioselectivity of a diimine Ni catalyst is quite temperature dependent.[16] At −78 °C, regioregular syndiotactic poly(propylene) (rr triads = 80%) is obtained, whereas at 0 °C a regioirregular polymer with slight syndiotacticity is obtained. Coates has reported a C_2-symmetric diimine catalyst that polymerizes propylene in a living fashion at −78 °C to yield highly isotactic polypropylene.[17] At higher temperatures regioirregular polypropylene is observed, and di- and triblock polymers can be prepared by simple temperature variation during polymerization. Kinetics of the polymerization of 1-hexene by a nickel catalyst activated with MAO were studied by Craimail.[18] While he describes the system as having two types of active propagating species, they are the differing isomers of the alkyl species and are consistent with our description of a single catalytic species residing at differing locations on the polymerized backbone. Finally, Sivaram has reported a very detailed ^{13}C study of Ni-diimine-catalyzed polymerization of 1-hexene and concluded that insertion of olefin into secondary nickel−alkyl bonds is an essential feature of certain nickel-catalyzed polymerizations.[19] These results are in substantial agreement with our earlier reports[20,21] and the work contained herein. There are, however, particular portions of the NMR assignments where we are in closer agreement with Freche,[22] and those assignments affect the proposed mechanism. We note that the nature of the resulting polymer displays a substantial dependence upon the nature of the catalyst, both on the metal and on the nature of the ligands on the metal. This report provides additional detail on the use of NMR spectroscopy coupled with ^{13}C labeling studies to gain additional mechanistic information regarding the enchainment mechanisms of higher α-olefins.

† Contribution No. 8499 from DuPont Central Research and Development.

* Corresponding authors. E-mail: elizabeth.f.mccord@usa.dupont.com; steven.d.ittel@usa.dupont.com; brookhar@email.unc.edu.

10.1021/ma061547m CCC: $37.00
Published on Web 01/06/2007

Scheme 1

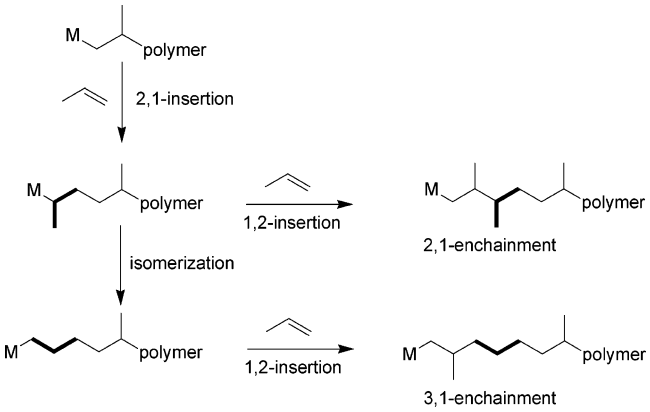

In contrast to late metal catalysts, polymerization of α-olefins by conventional Ziegler−Natta catalysts[23] and metallocene catalysts[24,25] generally give regioregular atactic or isotactic polymers via 1,2-insertion, but other modes of enchainment have been achieved using specially designed ligands. Syndiotactic polypropylenes[26−28] and higher poly-α-olefins[29] as well as more complicated stereochemistries[30] have been observed. It is well established that in isotactic polymerization of propene by metallocene catalysts there are occasional inversions of the normal 1,2-insertion to give 2,1-insertion. The essential features are delineated in Scheme 1.

A 2,1-insertion can lead to a 2,1-enchainment, or the 2,1-insertion can be followed by a isomerization that results in 1,3-enchainment (Scheme 1). With metallocene catalysts, both 1,3- and 2,1-enchainments have been observed as isolated regioerrors.[26] However, even with catalysts that give up to 24 mol % 1,3-enchainment of propene, there are no adjacent 1,3-enchainments.[31] A study of regiospecificity of 1-butene polymerization by a C_2-symmetric metallocene catalyst showed 1,4-enchainment but no evidence of 2,1- or 3,1-enchainment.[32] Apparently, in this case the intermediates formed by 2,1-insertion are too crowded for further olefin insertion and must rearrange to the primary alkyl species that leads to 1,4-enchainment. The process of isomerization, dubbed "chain walking", is far more facile with the late metal catalysts described herein.

Experimental Section

General Considerations. All manipulations of air- and/or water-sensitive compounds were performed using standard Schlenk techniques. Argon and nitrogen were purified by passage through columns of BASF R3-11 catalyst (Chemalog) and 4 Å molecular sieves. Solid organometallic compounds were transferred in an argon-filled Vacuum Atmospheres drybox. ^{1}H NMR spectra for the organometallic synthesis and the ^{13}C-labeled polymers were recorded with a Bruker AMX-300 spectrometer. Others were recorded as noted. ^{1}H NMR spectra of poly(olefins) were obtained in $CDCl_3$ or C_6D_5Br using a 15 s delay time. Gel permeation chromotography (GPC) was performed using a Waters HPLC vs polystyrene standards. Thermal analysis was performed on a Seiko Instruments DSC220C differential scanning calorimeter.

Materials. All solvents were deoxygenated and dried via passage over a column of activated alumina,[33] distilled under nitrogen from sodium benzophenone ketyl, or distilled from P_2O_5 in the case of methylene chloride. Chloroform-*d* and bromobenzene-d_5 were dried over 4 Å molecular sieves. 1-Hexene was purchased from Aldrich, and *cis*-2-hexene and *cis*-3-hexene were purchased from Acros. While not used in the polymerizations we describe here, these internal hexenes were used as references to chromatographically monitor any isomerization of the α-olefin to internal olefins during the course of the polymerizations.[21] This isomerization was observed in a number of polymerizations, particularly with palladium catalysts, and it was observed in polymerizations of the ^{13}C-labeled 1-hexene with palladium.[21] It was not observed in any of the polymerizations reported here but is a complication that must be considered when relating observed polymer structures to potential polymerization mechanisms. Why isomerization occurred with some olefins or olefins from some sources but not with others was never fully understood. The olefins were purged with argon and used without further purification. A 10% solution of MAO in toluene from Aldrich was used for activation of nickel dibromide complexes. The diimine ligands were prepared based on literature procedures.[4,6,34] The nickel dibromide complexes, (Ar−N═C(An)−C(An)═N−Ar)$NiBr_2$ (Ar = 2,6-C_6H_3(*i*-Pr)$_2$ and 2-C_6H_4(*t*-Bu)),[34] and cationic palladium complexes, [(ArN═C(R)−C(R)═NAr)Pd(CH$_3$)(OEt$_2$)]$^+$BAr′$_4^-$ (R = H, Me, or R,R = An; Ar = 2,6-C_6H_3(*i*-Pr)$_2$, Ar′ = 3,5-$(CF_3)_2C_6H_3$), have been reported.[4,6] A detailed synthesis of ^{13}C-labeled 1-hexene is presented in the Supporting Information.

General Procedure for Polymerization of 1-Hexene-*2-*^{13}*C* Using Activated Ni Dibromide Complexes. To conserve labeled monomer, the general conditions for each run varied slightly depending on the concentration of monomer desired. However, runs were set up following exactly the same sequence of events each time. Standard solutions containing 4×10^{-6} mol of nickel catalyst **1a** or **1b** per mL of solvent were prepared on a 10 mL scale by dissolving the complexes in a minimal amount of 1,2-difluorobenzene and diluting with toluene.

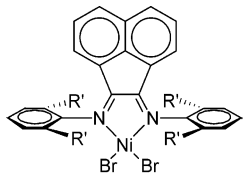

1a, 1b

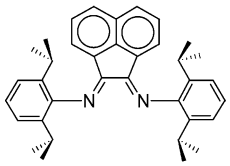

Ligand **a**

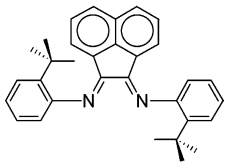

Ligand **b**

For a typical experiment, a 25 mL round-bottom Schlenk flask was charged via syringe with toluene, 1-hexene, and 200 equiv of MAO (10% solution in toluene). Polymerization was initiated immediately upon introduction of the standard catalyst solution (via gastight syringe) and was quenched through addition of 6 M HCl and acetone. The volatile components were removed under vacuum, and the remaining polymer was dissolved in hexanes and precipitated in acetone. The precipitated polymer was collected with a spatula, washed with water and acetone in a beaker, and dried under vacuum overnight. Analysis by GC of the volatile components removed under vacuum indicated no significant isomerization to internal olefins (<1%). The polymerizations are summarized subsequently.

NMR Analysis of the Labeled Polymers. Labeled polymers were dissolved in a 0.05 M solution of $Cr(acac)_2$ (relaxation agent) in 1,2,4-trichlorobenzene (ca. 5−15% w/v) with addition of ca. 10% bromobenzene-d_5 for establishment of a maintainable lock signal. Spectra were acquired with ^{1}H gated decoupling to reduce NOE enhancement using a 90° pulse at 110 °C with a 1 s acquisition time and a 10 s relaxation delay between scans.[11] Signals arising from natural abundance ^{13}C were assumed to be insignificant and were not taken into account in the analysis of the poly(1-hexene-*2-*^{13}*C*) samples. Signals for methylene and methine carbons were determined from DEPT experiments. Note that in the ^{13}C-labeled

experiments the numbers reported are branching density, reported as branches per 1000 carbon atoms.

Polymerizations of α-Olefins with Pd Catalysts. Polymerization of 1-Pentene. The Pd complex catalyst **2**, $PdCH_2CH_2CH_2C(O)OCH_3[((2,6\text{-}i\text{-}Pr\text{-}C_6H_3)N{=}CMe)_2)]^+SbF_6^-$, was loaded into a tared round-bottom flask in the drybox, and 20 mL $CHCl_3$ was added, followed by 20 mL of 1-pentene. The mixture was stirred in the drybox for 3 days and then worked up by stripping off the solvent and unreacted monomer to give 2.59 g of viscous fluid (370 equiv of 1-pentene per Pd). Integration of the ^{1}H NMR spectrum showed 118 methyl carbons per 1000 methylene carbons. DSC (two heats, −150 → 150 °C, 15 °C/min) shows $T_g = -58$ °C and a low-temperature melting endotherm from −50 to 30 °C (32 J/g). ^{13}C NMR quantitative analysis, branching per 1000 CH_2: total methyls (118), methyl (85.3), ethyl (none detected), propyl (15.6), butyl (none detected), ≥amyl and end of chains (17.1). GPC (trichlorobenzene, 135 °C, polystyrene reference, results calculated as linear polyethylene using universal calibration theory): M_n = 22 500, M_w = 43 800, M_w/M_n = 1.94. Integration of the CH_2 peaks due to the structure −CH(R)CH_2CH(R′)−, where R is an alkyl group and R′ is an alkyl group with two or more carbons, showed that in 69% of these structures R = Me. The region integrated for the structure where both R and R′ are ≥ethyl was 39.7−41.9 ppm to avoid including an interference from another type of methylene carbon on a side chain.

Polymerization of 1-eicosene (19.0 g) was carried out in methylene chloride (15 mL) for 24 h using catalyst **2** (0.047 g, 0.05 mmol). The solvent and unreacted monomer were removed in vacuo. The polymer was reprecipitated to remove residual monomer by addition of excess acetone to a chloroform solution of the polymer. The solution was filtered to collect the polymer. The filtered polymer was dried in vacuo to give 5.0 g of fluffy white powder. ^{13}C NMR quantitative analysis, branching per 1000 CH_2: total methyls (27), methyl (14.3), ethyl (0), propyl (0.2), butyl (0.6), amyl (0.4), ≥hexyl and end of chains (12.4). Integration of the CH_2 peaks due to the structure −CH(R)CH_2CH(R′)−, where R is an alkyl group and R′ is an alkyl group with two or more carbons, showed that in 82% of these structures R = Me.

1-Hexene was polymerized in a manner similar to the eicocene to give a viscous gel (1000 equiv of 1-hexene per Pd). Integration of the ^{1}H NMR spectrum showed 95 methyl carbons per 1000 methylene carbons. ^{13}C NMR quantitative analysis, branching per 1000 CH_2: total methyls (103), methyl (74.9), ethyl (none detected), propyl (none detected), butyl (12.4), amyl (none detected), ≥hexyl and end of chains (18.1). Integration of the CH_2 peaks due to the structure −CH(R)CH_2CH(R′)−, where R is an alkyl group and R′ is an alkyl group with two or more carbons, showed that in 74% of these structures R = Me.

1-Heptene (20 mL) was polymerized in a manner similar to the eicocene to give a viscous gel (260 equiv of 1-heptene per Pd). Integration of the ^{1}H NMR spectrum showed 82 methyl carbons per 1000 methylene carbons. ^{13}C NMR quantitative analysis, branching per 1000 CH_2: total methyls (85), methyl (58.5), ethyl (none detected), propyl (none detected), butyl (none detected), amyl (14.1), ≥hexyl and end of chains (11.1). Integration of the CH_2 peaks due to the structure −CH(R)CH_2CH(R′)−, where R is an alkyl group and R′ is an alkyl group with two or more carbons, showed that in 71% of these structures R = Me. DSC (two heats, −150 to 150 °C, 15 °C/min) shows $T_g = -42$ °C and a $T_m = 28$ °C (45 J/g).

1-Octadecene was polymerized in a manner similar to the eicocene to give a fluffy white powder (520 equiv of 1-octadecene per Pd). ^{13}C NMR quantitative analysis, branching per 1000 CH_2: total methyls (37.4), methyl (19.5), ethyl (none detected), propyl (0.2), butyl (none detected), amyl (2.9), ≥hexyl and end of chains (17.5). DSC (two heats, −150 to 150 °C, 15 °C/min) shows $T_g = -8$ °C and a $T_m = 66$ °C (102.3 J/g).

NMR Analysis. ^{13}C NMR spectra of the polymers prepared with the Pd catalysts were obtained on a Varian Unity 400 MHz spectrometer on 20 wt % solutions of the polymers and 0.05 M $Cr(acac)_3$ in 1,2,4-trichlorobenzene (TCB) unlocked at 120−140 °C using a 90° pulse of 12.5−18.5 μs, a spectral width of 35 kHz, a relaxation delay of 5 s, an acquisition time of 0.64 s, and inverse gated decoupling. Samples were preheated for at least 15 min before acquiring data. Data acquisition time was typically 12 h per sample. The T_1 values of the carbons of a branched polyethylene sample were measured under these conditions and found to be all less than 0.9 s. The longest T_1 measured was for the Bu^+, EOC resonance at 14 ppm, which was 0.84 s. Spectra are referenced to the TCB high-field resonance at 127.918 ppm.

Integrals of unique carbons in each branch ($1B_2$, $2B_3$, $1B_1$, $2B_4$, $3B_5$, and $3B_{6+}$, 3EOC) were measured and were reported as number of branches per 1000 methylenes, including methylenes in the backbone and branches. These integrals are accurate to ±5% relative for abundant branches and ±10% or ±20% relative for branches present at less than 10 per 1000 methylenes. Note that the numbers reported are per 1000 methylene carbon atoms as opposed to the ^{13}C-labeled experiments, where the numbers reported are per 1000 total carbon atoms.

The 2D INADEQUATE experiment was run on a Varian VXR-S 400 MHz NMR spectrometer using a 10 mm BB probe. The sample was 1.7 g of poly(1-olefin) and 0.05 M $Cr(acac)_3$ (60 mg) with ODCB-d_4 in a total volume of 3.1 mL. The spectrum was run at 120 °C. To obtain the high resolution needed in a reasonable amount of time, the spectral width in the f_1 dimension was folded 1 time. Linear prediction was used to extend the data set in the f_1 dimension by a factor of 4. An additional factor of 4 was gained by zero filling 2×. A T_1 relaxation experiment was performed on this sample and showed that the T_1 values of the carbons were all less than 0.4 s under these conditions. A delay of 0.37 s, 9200 transients per increment, 64 increments, no homospoil, and an acquisition time of 0.18 were used. The INADEQUATE experiment took 4 days to complete under these conditions. Indirect detection experiments (hmqc, hmbc) were run on a Varian Unity 400 MHz spectrometer.

Nomenclature. The nomenclature system being employed is consistent with our previous publication on polypropylenes.[11] The ^{13}C NMR resonances are labeled according to the following naming scheme: xB_y: B_y is a branch of length y carbons; x is the carbon being discussed; the methyl at the end of the branch is numbered 1. Thus, the second carbon from the end of a butyl branch is $2B_4$. The term xB_y+ refers to branches of length y and longer. The methylenes in the backbone are denoted by a capital S and with Greek letters that determine how far from a branch point methine each methylene is. Thus, $S_{\beta\beta}$ denotes the central methylene in the following structure: RCHRCH_2CH_2CH_2CHRR. The term γ^+ refers to methylenes γ and further from a branch point. When x in xB_y is replaced by an M, the methine carbon of that branch is denoted. EOC indicates the methyl group at the end of the polymer chains and at the ends of any branches that are six or more carbon atoms in length.

Results

Palladium-Catalyzed Polymerizations. The palladium α-diimine complex, **2**, is a single-component catalyst for the addition polymerization of α-olefins. Complex **2** was chosen as the catalyst precursor for most of the polymerizations because it is thermally stable and is relatively insensitive to water or oxygen. Mechanistic studies establish the active species in the polymerization to be the cationic Pd alkyl complex with a π-bound olefin ligand (**3**).[4,12−14] The polymerization rates are moderate

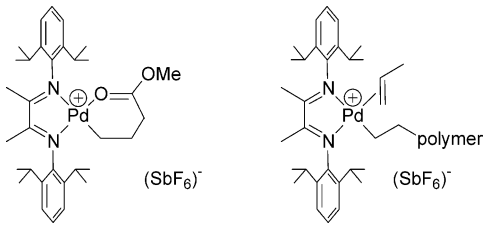

2 **3**

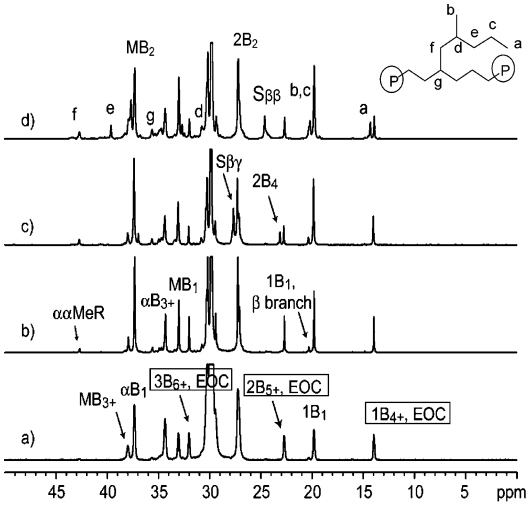

Figure 1. ^{13}C NMR spectra of polymers of (a) 1-eicosene, (b) 1-nonene, (c) 1-hexene, and (d) 1-pentene polymerized by catalyst **2**. Labels are explained in the text. The large peak at 30 ppm is $(CH_2)_n$. In this figure, common signals are only labeled on one of the four spectra for clarity. For example, $1B_1$, which is present in all four spectra, is only labeled in (a). Also, it should be noted that in (d) signals b, c, and $1B_1$ are overlapping in the 20 ppm region.

Scheme 2

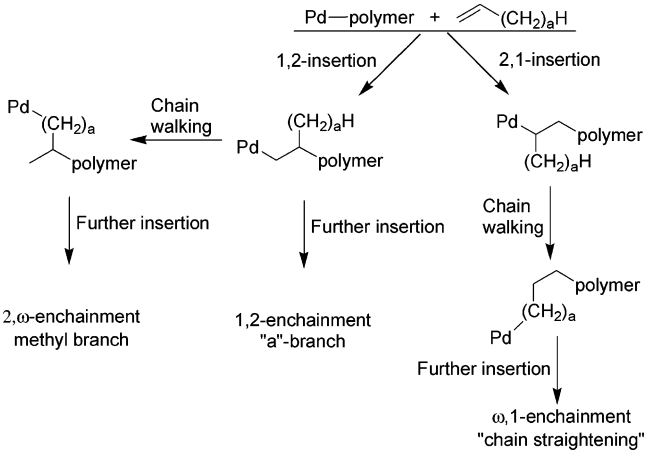

Table 1. Branching of Poly(α-olefin)s Made with Catalyst 2

no. of carbons in monomer	ω,1[a]	total Me	Me[b]	Et	Pr	Bu	Am	hexyl+
5	0.52	118	85		16			17
5	0.53	115	82		16			16
6	0.49	103	75			12		18
7	0.49	85	59				14	11
9	0.50	63	43					21
18	0.37	37	20		0.2		3	18
20	0.48	27	15				0.4	12
20	0.41	31	18					12
20	0.44	30	17	0.1				15

[a] The fraction of ω,1-insertions. The term ω,1 implies that an olefin has inserted and then chain-walked to give an insertion that is through the ω and 1 carbon atoms. See Scheme 2. [b] The Me numbers are Me groups/1000 methylenes. Total Me's essentially equals the sum of Me's on all the branches with end-group methyls making an insignificant difference.

at room temperature, typically in the range of 10−100 turnovers/h. Linear α-olefins from C_5 to C_{20} were polymerized with this catalyst. The branching of the polymers was characterized by ^{1}H NMR spectroscopy for total branching level and ^{13}C NMR spectroscopy for quantification of individual branch levels. Figure 1 shows the ^{13}C NMR spectra for polymers of 1-pentene, 1-hexene, 1-nonene, and 1-eicosene.

Most of the poly(α-olefin)s made with catalyst **2** show three major branch lengths: methyl branches, "*a*" branches ($a + 2$ = number of carbons of the α-olefin), and ≥hexyl branches (Table 1). For example, poly(1-pentene) has a very specific branching pattern with no detectable ethyl, butyl, or amyl branches.

The total quantity of branching and the distribution of branches can be explained by Scheme 2 that shows the mechanism of α-olefin polymerization by the palladium catalyst and three mechanistic "rules": (1) Both 1,2- and 2,1-insertions can occur. (2) Chain-walking of the metal down the hydrocarbon chain occurs via a sequence of β-hydrogen elimination/readdition reactions. The rate of chain-walking is faster than olefin insertion. (3) Insertion occurs only into primary Pd−alkyl bonds. Each of these "rules" will be discussed at greater length later.

Scheme 3 shows all of the possible diad structures for 1-pentene polymerization using this mechanism. The notations

Scheme 3

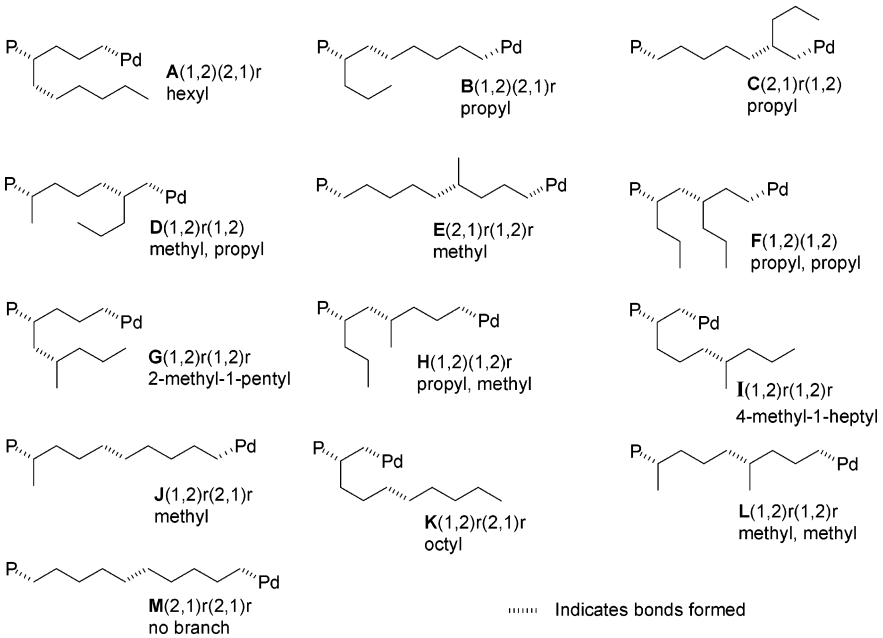

(1,2) or (2,1) indicate the nature of insertions, and the notation "r" indicates that the catalyst has migrated or chain walked to a new position between insertions. As will be discussed later, the notation of consecutive insertions implies "effective" consecutive insertions but does not necessitate that the catalyst has not chain walked to a new position and then returned to the site of the next insertion. Scheme 3 illustrates how the mechanistic model leads to the specific branches methyl, "*a*" branches (in this case propyl), and ≥hexyl branches.

The mechanistic model of Scheme 2 allows for a quantitative analysis of the fraction of ω,1-enchainment based on the total branching in the polymer:

$$x_{\omega,1} = \text{fraction of } \omega,1\text{-enchainment}$$

$$(a+2) = \text{total number of carbon atoms in the monomer}$$

$$B = \text{total branching per 1000 methylene carbon atoms}$$

$$B = \frac{1000(1-x_{\omega,1})}{(1-x_{\omega,1})a + x_{\omega,1}(a+2)}$$

Solving for $x_{\omega,1}$ gives

$$x_{\omega,1} = \frac{1000 - aB}{1000 + 2B}$$

Looking at the subset of the data in Table 1, the fraction of ω,1-enchainment (from 2,1-insertion) ranges from 0.41 to 0.53 and does not depend significantly upon monomer. Thus, catalyst **2** does not have a significant selectivity for 1,2- vs 2,1-insertion.

Chain-walking is an important feature of the formation of highly branched polyethylene by the palladium catalyst **2**. A significant difference between the mechanism of ethylene polymerization and α-olefin polymerization with this catalyst is that ethylene can insert into secondary Pd−alkyl bonds, whereas α-olefins are observed to insert only into primary Pd−alkyl bonds. The reasons for this selectivity are discussed below.

According to Scheme 3, two branch-on-branch structures are expected among the diads of poly(1-pentene). ^{13}C NMR resonances consistent with the expected 2-methylpentyl branch of poly(1-pentene) were detected (see the 1B1β branch noted in Figure 1). This structure can be accounted for by a sequence of two 1,2-insertions followed by a chain-walking back to the end of the first inserted 1-pentene:

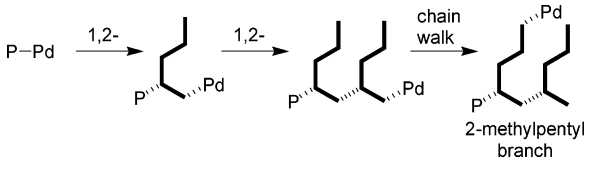

The expected 4-methyl-1-heptyl branch (**I**, Scheme 3) is indistinguishable from normal branching (i.e., comb-type structures) by ^{13}C NMR chemical shifts under our experimental conditions. The significant level of 2-methylpentyl branching in poly(1-pentene) suggests the possibility that these polymers may have hyperbranched structures.

Previous mechanistic studies of migratory insertions in diimine palladium alkyl ethylene complexes support the presumed hyperbranched structures of poly(α-olefins) and provide considerable information with respect to α-olefin enchainment.[12−14] Key results of these studies are summarized below for the model system involving ethylene insertion into the butyl group in complexes **4a** and **4b** in Scheme 4.

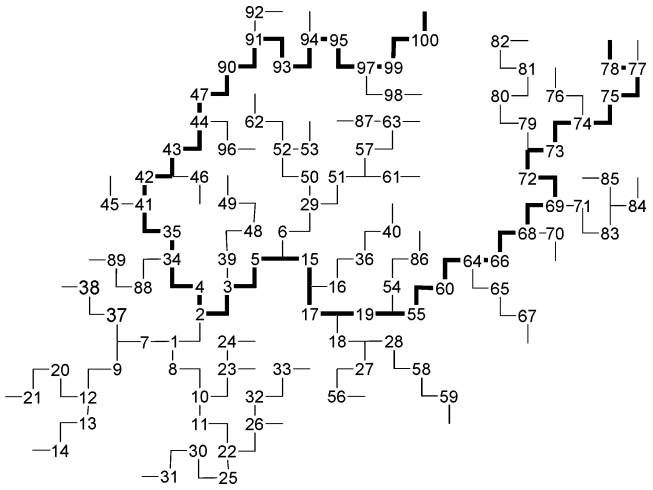

Figure 2. Simulated structure of polyethylene produced with catalyst **2**.

The rate of equilibration of the primary and secondary alkyl ethylene complexes, **4b** and **4a**, was shown to be extremely rapid relative to their rates of migratory insertion (k_1, $k_{-1} \gg k_{\text{ins,l}}$, $k_{\text{ins,2}}$). Thus, the ratio of primary to secondary insertion products, P(l):P(2), is given by $K_{\text{eq}}(k_{\text{ins,1}}/k_{\text{ins,2}})$ and follows Curtin−Hammett kinetics. In the case shown above, the equilibrium favors the primary alkyl ethylene complex, **4b**, $K_{\text{eq}} \approx 11$ at −20 °C, but the barrier to insertion in the secondary alkyl complex, **4a**, is slightly lower than that for the primary alkyl ethylene complex, **4b**: $k_{\text{ins,2}}$:$k_{\text{ins,1}} \approx 2$. Thus, the polyethylene produced by the Pd diimine complex is branched, and the extent of branching is controlled not only by the relative rates of insertion into primary and secondary bonds but also by the equilibrium distribution of secondary and primary alkyl ethylene complexes, the resting states of the catalyst. Furthermore, we have shown that although tertiary agostic alkyl complexes are energetically accessible, no insertion occurs into tertiary bonds since tertiary alkyl ethylene complexes are highly disfavored energetically.

These observations explain why polyethylenes produced from Pd complexes exhibit hyperbranched structures since Pd can readily migrate through a 3° carbon (branch point) formed from insertion of ethylene into a secondary palladium alkyl bond. The ethylene alkyl complexes equilibrate via ethylene dissociation followed by isomerization (β-elimination, olefin rotation, reinsertion) of the agostic metal alkyl complex, and thus the rate of isomerization can be retarded by high ethylene concentrations. This implies that the average number of carbons over which Pd migrates prior to insertion decreases with ethylene pressure and explains the observation that as ethylene pressure is increased the PE produced moves from a hyperbranched architecture to a more linear but still highly branched architecture.[35]

Graphical illustration of the consequences of the mechanistic features described above is depicted in Figure 2, which shows a model structure of a polyethylene (100 ethylene insertions) prepared using catalyst **2**. The statistical model, developed to explain the observable structures of a wide range of Versipol polyethylenes, gives very good fits to the polyethylene structures described in previous papers.[36] Similar results have been obtained from other computational techniques.[37−39] Using the known branching distribution of the polyethylene generated from catalyst **2**, artificial intelligence was used to determine the

Scheme 4

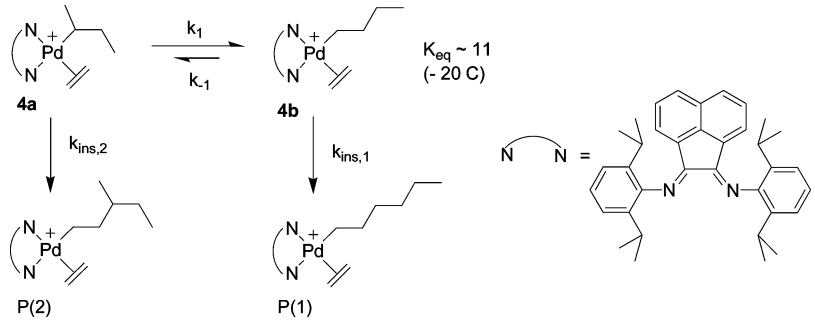

relative rates of all possible chain-walking and insertion events in the polymerization process under the conditions used to form a particular structure.

The resulting model polyethylene (100 molecules of ethylene incorporated) is obviously highly branched. The numbers on the carbon atoms signify the sequence of insertions of the consecutive monomers. The bold bonds indicate the longest observed backbone sequence in the structure. The polymerization was initiated in the lower left where insertions 1−6 are clearly adjacent. However, note that insertion 34 occurred at the fourth ethylene and that insertion 88 occurred at the 34th ethylene. Clearly there was considerable chain-walking and ethylene insertion between the 4th, 34th, and 88th insertions. The catalyst was required to chain walk through tertiary centers to achieve this structure and is consistent with mechanistic observations.

The above observations concerning ethylene insertion result in the following deductions concerning α-olefin enchainment:

A. The equilibrium between a primary alkyl α-olefin complex (for example, **5b**) and a secondary alkyl α-olefin complex (for example, **5a**) should very strongly favor the primary alkyl complex based on the larger steric bulk of an α-olefin compared to ethylene:

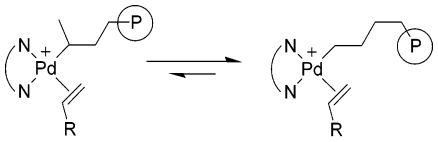

B. The rates of equilibration of primary and secondary alkyl α-olefin complexes (e.g., **5b** and **5a**) should be *much* faster than for ethylene complex analogues due to the weaker binding affinity of the bulkier α-olefins.

Features A and B, coupled with our previous observation that the barrier for insertion of propylene into a palladium methyl bond is somewhat higher than the analogous ethylene insertion barrier, imply that insertion of an α-olefin will occur virtually exclusively into primary palladium−alkyl bonds because these complexes have even more time to equilibrate among various isomers prior to insertion. Furthermore, these results indicate that Pd will, on average, chain walk over a very large number of carbon atoms on the polymer chain prior to insertion, and thus hyperbranched polymers will be formed from α-olefins using Pd diimine catalysts. These results are supported by our studies of the properties of block copolymers of α-olefins formed from palladium diimine catalysts.[40]

Microstructural Implications of the Mechanistic Model

A particular set of backbone microstructures are expected to result from the mechanistic model described in the previous section. Thus, characterization of backbone microstructure allows further testing of this model. The number of methylene units between branches should be dependent upon the monomer. Scheme 5 shows those predictions of the backbone microstructure. For a given monomer with $(a + 2)$ carbon atoms, two series of backbone $-CH(R)(CH_2)_nCH(R)-$ structures can be formed. The beginning and end of the $-CH(R)(CH_2)_nCH(R)-$ structures are defined by 1,2-insertions that produce methine carbon atoms. Intervening 2,1-insertions add linear $(CH_2)_{a+2}$ fragments, thus contributing the $y(a + 2)$ term (y = an integer).

Scheme 5

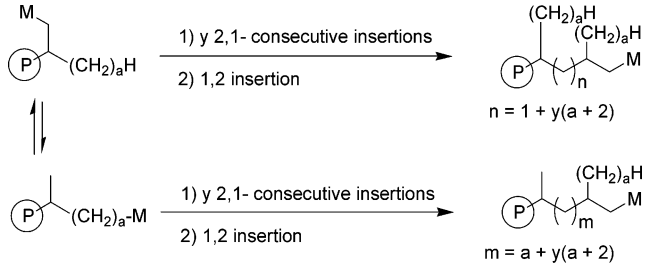

Olefin	a =	n =	m =
Butene	2	1, 5, 9, …	2, 6, 10, …
Pentene	3	1, 6, …	3, 8, …
Hexene	4	1, 7, …	4, 10, …
Heptene	5	1, 8, …	5, 12, …

^{13}C NMR spectra confirm the predicted unique backbone microstructures for polymers of 1-pentene and 1-hexene. The two microstructures contain β,β and β,γ units.

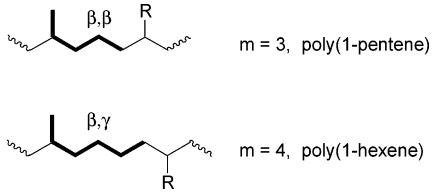

There are an increasing number of methylenes between the methyl and alkyl branch points. All spectra also show a peak for δ^+-methylenes due to n, $m \geq 6$ resulting from additional linear insertions; this is essentially a linear polyethylene component.

The backbone microstructure $-CH(R)CH_2CH(R')-$ (i.e., $n = 1$) is a special case. Since the initiating branch for this structure originates from a 1,2-insertion without chain-walking, one of the R groups is always greater than methyl. The second R group can be either methyl (1,2-insertion followed by chain-

walking) or greater than methyl (1,2-insertion without chain-walking). The high level of Me branches in polymers made with Pd catalysts suggests that after a 1,2-insertion more than 50% of the time there is chain-walking before further insertion. The three possible α,α-methylene carbons have distinctive chemical shifts.

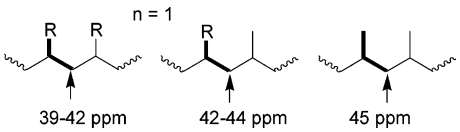

As a result, ^{13}C NMR can be use to determine the relative amounts of these structures. None of the poly(α-olefin)s made with catalyst **2** show a resonance at 45 ppm. The major signals for the α,α-methylene carbons occur in the 42−44 ppm range. At first glance poly(1-pentene) does not appear to fit this order, but closer analysis shows that the major peak in the 39−42 ppm region is due to a unique branch-on-branch structure (Figure 1). It is quite striking that even though methyl branches are the most common branches, none of the polymers contain an α,α-methylene carbon atom between two methyl branches (~45 ppm). The −CH(R)CH_2CH(Me)− structure (R > Me, 42−44 ppm) seems to be unique to the polymers made with these catalysts and is not normally found in poly(α-olefins) made with other catalysts.

At room temperature these polymers range from amorphous elastomers to low-melting partially crystalline solids (Table 2). The melting points and heats of fusion both correlate with the length of the monomer. This is consistent with crystallization of runs of methylene groups in the backbone formed by consecutive *ω*,1-enchainments (i.e., chain straightening). As the monomer size increases, the average length of these methylene runs increases, thereby increasing the T_m. The low-temperature endotherm for poly(1-pentene) is reminiscent of the melting behavior of "amorphous" polyethylene made with this catalyst. This polyolefin has a broad melting endotherm centered at −37 °C (8.3 J/g) that may be attributed to backbone crystallinity of $-(CH_2)_n-$ segments.

Nickel-Catalyzed Polymerizations. The enchainment mechanism observed when α-olefins are polymerized using Ni diimine catalysts was investigated in detail employing catalysts **1a** and **1b**. The olefins studied were 1-hexene and 1-hexene labeled with ^{13}C (99%) in the 2-position, $CH_2{=}^{13}CH(CH_2)_3CH_3$, designated throughout as 1-hexene*. Polymerizations were carried out at 0, 25, and 55 °C in 10 vol % 1-hexene; catalysts were activated with ca. 200 equiv of MAO. Turnover frequencies fell in the range of 1000−2000 turnovers/h with M_n values in the range 40K−90K. Molecular weight distributions were monomodal and ranged, for example, for catalyst **1a** from 1.15 (0 °C) to 2.08 (55 °C), clearly indicating a single site catalyst.

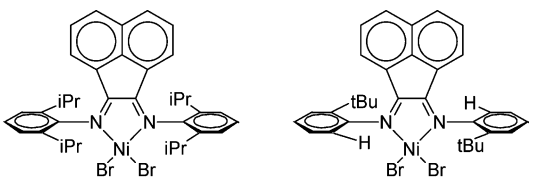

1a **1b**

The ^{13}C NMR spectra of unlabeled poly(1-hexene) produced from catalysts **1a** and **1b** at 25 °C are shown in Figure 3, and the assignments are shown in Scheme 6. ^{13}C NMR assignments were made by combining the results of DEPT experiments,

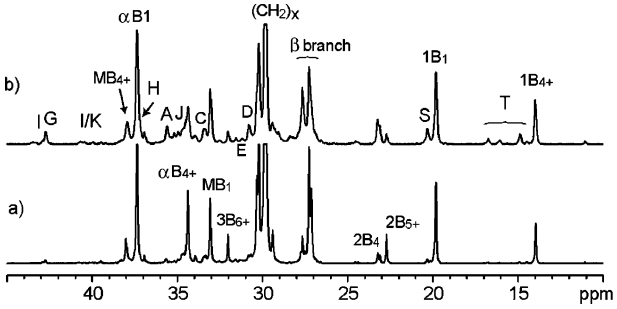

Figure 3. ^{13}C NMR spectra of polymer from 1-hexene polymerized using catalysts **1b** (a) and **1a** (b). See Scheme 6 for assignments; R indicates alkyl groups longer than methyl.

Table 2. DSC of Poly(α-olefin)s

sample	T_g (°C)	T_m (°C)	ΔH (J/g)
poly(1-pentene)	−58	5	32
poly(1-heptene)	−42	28	45
poly(1-octadecene)	−8	66	102

Scheme 6

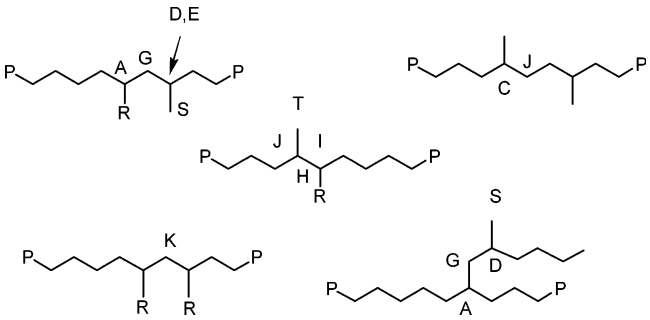

chemical shift calculations using empirical tables of substituent effects, and reference to model compound data found in the NMR literature. Note that for Scheme 6 P is the continuing polymer chain and R indicates an alkyl chain longer than methyl. Comparing the ^{13}C NMR spectra of unlabeled poly(1-hexene) produced from catalysts **1a** and **1b** shown in Figure 3 with those of poly(1-hexene) produced from a palladium diimine catalyst **2** (Figure lc) reveals that, qualitatively, they are quite similar. Short-chain methyl and butyl branches can be identified by $1B_1$ and $2B_4$ resonances at 20 and 23 ppm; amyl and longer branches are present as shown by the substantial $1B_{4+}$ signal at 14 ppm and, for example, the $2B_{5+}$ band at 22.7 ppm. There are no detectable ethyl and propyl branches as evidenced by lack of a $1B_2$ methyl resonance at 11 ppm and a $2B_3CH_2$ resonance at 20 ppm (no CH_2 detected by DEPT). One significant difference between poly(1-hexene) prepared from Pd catalyst **2** and Ni catalyst **1b** vs poly(1-hexene) prepared from **1a** is the occurrence of methyl signals marked T for the latter polymer (see Figure 3b). These are due to adjacent methyl branches as well as methyls adjacent to longer branches and must arise from a small fraction of 1,2 insertion of 1-hexene into secondary alkyl bonds. Sivaram assigns all of these T peaks to methyl−methyl adjacency.[19] These resonances are certainly due to methyl branches adjacent (alpha) to other branches. However, the Sivaram paper assumes that these are due only to adjacent methyl to methyl branches whereas we believe at least some of these arise from methyl groups adjacent to butyl branches. Our arguments are supported by the 43 ppm methine signal. Sivaram indicates that a *γ*-methyl branch is responsible for a change in shift from 38 to 43 ppm. We expect such a branch to give a 0.6 ppm increase in the chemical shift, not 5 ppm. Our alternative explanation that this is the methine of an R group adjacent to

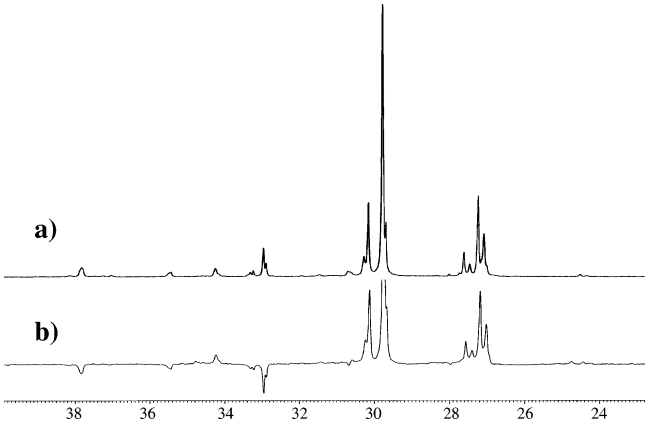

Figure 4. (a) ^{1}H-decoupled ^{13}C NMR spectrum and (b) DEPT spectrum (−CH− = down; $-CH_2-$ = up) of poly(1-hexene*) made via 1b/MAO catalysis.

a methyl branch is reasonable. Freche[22] indicates that for the structure

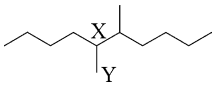

methine X will be at 37.15 and 38.12 ppm, while methyl Y will appear at 14.69 and 16.75 ppm (two values indicating the stereoisomers), while in the structure

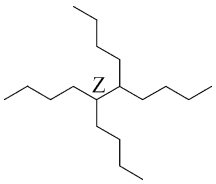

methine Z will be observed at 40.13 ppm (only one isomer was given). On the basis of these examples, our assignment of

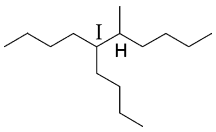

is about 42 ppm for I and 35−36.5 ppm for H, values that are in accord with our spectra.

Thus, from examination of these spectra, the mechanism of enchainment shown in Scheme 2 for the palladium diimine catalysts (referred to here as the first generation mechanism) would appear to be appropriate for the Ni systems as well with the exception of a small fraction of secondary 1,2 insertion occurring for catalyst **1a**. However, analysis of ^{13}C spectra obtained for poly(1-hexene*) requires the modification of this mechanism as described below.

1-Hexene* (10 vol %, 0.8 M, in toluene) was polymerized using both catalysts **1a** and **1b** activated with MAO. The ^{13}C spectrum of poly(l-hexene*) produced using catalyst **1b** is shown in Figure 4. The DEPT spectrum in Figure 4b reveals the methine carbons as inverted signals. Resonances arising from natural abundance ^{13}C are assumed to be negligible since the monomer is enriched at the 99% level. Each resonance can be assigned to a structure consistent with a polymer produced via the first generation mechanism, with the exception of the group appearing between 27.0 and 27.7 ppm. These same resonances,

Scheme 7

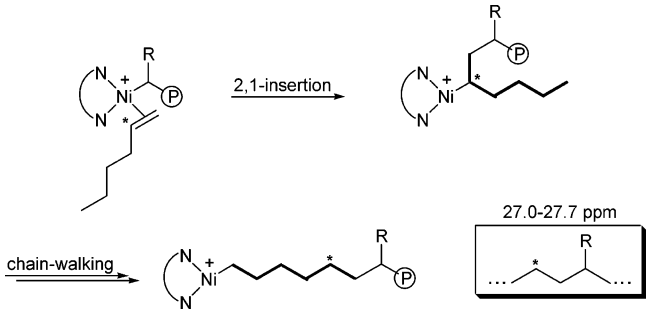

although less pronounced, appear in the poly(1-hexene) produced from **1b**/MAO and are uniquely assigned to methylene carbons β to a branch in a polymer chain. Placement of ^{13}C β to a branch from either 1,2- or 2,l-insertion of 1-hexene* into a l° Ni−alkyl bond via the first generation mechanism is not possible. ^{13}C placement β to a branch must occur via 2,l-insertion of 1-hexene* into a 2° Ni−alkyl bond followed by chain-walking away from the labeled carbon, as shown in Scheme 7. Furthermore, the fact that *no ethyl or propyl branches are detected indicates that R in Scheme* 7 *must be a methyl group*. (The reason for this restriction will be addressed below.) As noted above, with catalyst **1b**, the secondary Ni−alkyl intermediates do not undergo 1,2-insertion, but the appropriate resonances are observed in the polymer from catalyst **1a**. However, evidence for a small fraction of secondary 1,2 insertion in the labeled polymer prepared from **1a** can be seen from the appearance of a low-intensity resonance at 37.5 ppm assigned to H and upfield from the mB^{+}_{4} resonance (see the Supporting Information). This is consistent with the appearance of T resonances in the unlabeled polymer (Figure 3a).

The first generation mechanism predicts only 1,2-, 2,6-, and 1,6-enchainments of 1-hexene (Scheme 2) with formation of methyl and butyl branches (branches longer than five carbon atoms can be formed from chain-walking; see Scheme 2). On the basis of the labeling results, we must now add 1,5- and 2,5-enchainment modes which give rise exclusively to methyl branches. The revised mechanism for enchainment of 1-hexene* for Ni systems is summarized in Scheme 8. In the initial mechanism, every 1,2-insertion gave rise to a single branch while every 2,l-insertion resulted in no incorporation of branches due to metal migration to a primary carbon atom prior to the next insertion. Thus, the fraction of 1,2-insertions was readily predicted from the total branches per 1000 carbons calculated from the ^{1}H NMR spectrum by eq 1:

$$\%\ 1,2\text{-insertion} = \frac{n\ \text{branches}}{1000\ \text{C}} \frac{1\ (1,2)}{1\ \text{branch}} \frac{1000\ \text{C}}{166.7\ \text{insertions}} \times 100 \quad (1)$$

where n branches was determined from the ^{1}H NMR spectrum and (1,2) = 1,2-insertion. With the modified Scheme 8, a 1,2-insertion gives at least one branch (1,2- or 2,6-enchainments from C or A) and at most two branches (2,5-enchainment from H), while a 2,l-insertion leads to incorporation of either zero (1,6-enchainment from F) or one (1,5-enchainrnent from E) branch. The actual percentages of 1,2- vs 2,l-insertions can be directly determined from the ratio of methine and methylene integrals in the ^{13}C spectrum of poly(1-hexene*) since every 1,2-insertion results in the generation of a methine ^{13}C and every 2,1-insertion results in a methylene ^{13}C. Since all branches result from either 1,2-insertions or 2,l-insertions into a secondary Ni−

Scheme 8

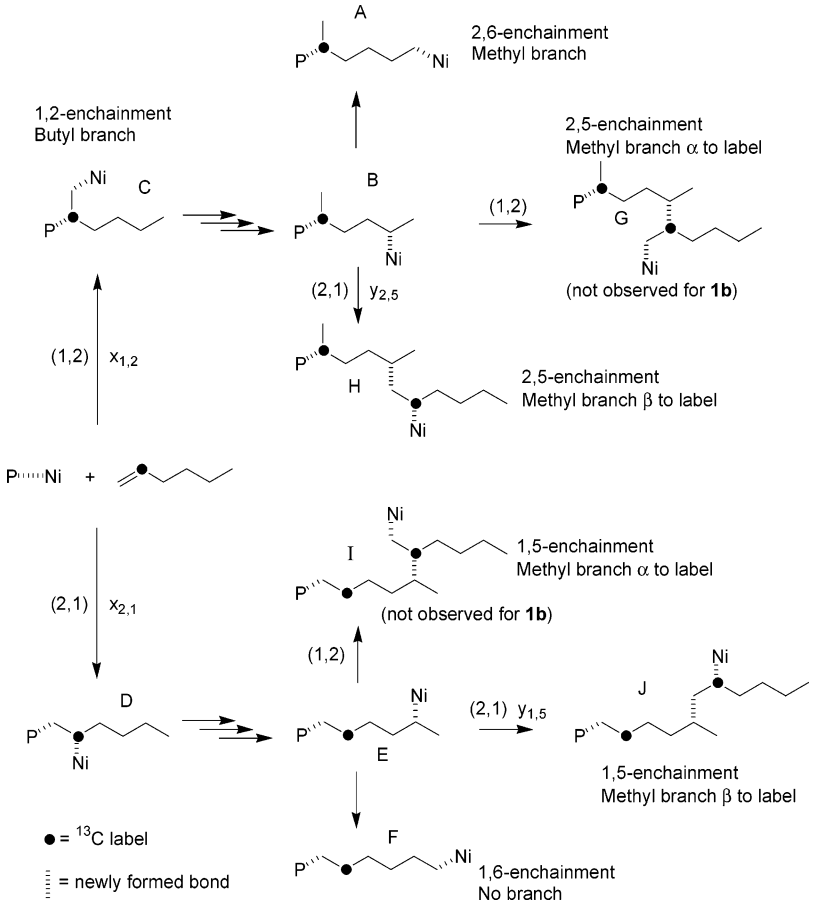

Table 3. Branching and Insertion Data for Poly(1-hexene-*2*-^{13}C) Made via Activation of Nickel Complexes

	branches/1000C		% 1,2-:2,1-insertion	
complex	^{1}H NMR[a]	^{13}C NMR[b]	predicted[c]	actual[d]
1a	119	112	71:29	57:43
1b	63	76	36:64	14:86

[a] Calculated from ratio of methyl carbons to all carbons as determined from the ^{1}H NMR spectrum. [b] Calculated from integrals of labeled methine carbons and methylene carbons β to a branch (eq 5.2). [c] Calculated based on initial mechanism for 1H branching count (eq 5.1). [d] Determined directly from sum of labeled methine vs sum of labeled methylene carbons.

alkyl bond, the total branches per 1000 C's based on the ^{13}C spectrum of the labeled polymer can be calculated from eq 2:

$$\frac{\text{branches}}{1000\ \text{carbons}} = \frac{[\%(1,2) + \%(2,1){:}2°]}{100\ \text{insertions}} \frac{166.7\ \text{insertions}}{1000\ \text{C}} \quad (2)$$

where %(1,2) = % 1,2-insertion determined from the sum of the methine integrals and %(2,1):2° = % 2,1-insertion into 2° Ni−alkyls determined from the integral of shifts between 27 and 28 ppm. Furthermore, since a 2,l-insertion into a secondary Ni−alkyl bond results in a *CH_2 β to a branch (27−28 ppm) while 2,l-insertion into a primary Ni−alkyl bond results in *CH_2 at least γ or further from a branch, the ratio of integrals at 27−28 ppm to all other methylene signals in the labeled polymer provides the ratio of 2,1/2° to 2,1/1°.

Table 3 compares the enchainment characteristics determined from both the ^{1}H and ^{13}C NMR data for poly(1-hexene*) formed by catalysts **1a** and **1b** at 25 °C. These independent analyses are in reasonable agreement. The third column in Table 3 shows the predicted ratio of 1,2- and 2,l-insertions based on the first generation mechanism (i.e., only 1,2-insertions result in formation of a branch). Column 4 shows the actual ratio of 1,2- vs 2,l-insertions determined from analysis of the labeled polymer. For both complexes, these ratios are significantly different. For example, for catalyst **1b**, there are 22% fewer 1,2-insertions (14% vs 36%) than predicted using ^{1}H data and the initial enchainment mechanism. If branching arose only from 1,2-insertions (first generation mechanism), the polymer produced from **5** would contain only ≈23 branches/1000 C, while polymer from **1a** would exhibit ≈95 branches/1000C. In the case of **1b**, considerably more than half the branches formed are a result of 2,1-insertions into secondary Ni−alkyl bonds.

Table 4 summarizes ^{13}C NMR data for labeled poly(1-hexene*) prepared at three different temperatures (0, 25, and 55 °C) with catalysts **1a** and **1b**. The ^{13}C data are used to calculate the % 1,2-insertions as well as to dissect the fraction of 2,l-insertions into 2,1-insertions occurring from primary alkyl species vs those occurring from secondary alkyl species.

The data show that as the polymerization temperature increases, the minor insertion pathways, as expected, increase at the expense of the major pathway. In the case of catalyst **1a**, the fraction of 1,2-insertion, the major insertion pathway, drops from 67% at 0 °C to 53% at 55 °C, which results in a decrease in branching, 127/1000C to 107/1000C. (A small increase in the fraction of 2,1/2° is not sufficient to compensate for the decrease in 1,2-branching.) For catalyst **1b**, the 1,2-insertion is a minor pathway and increases with temperature. However, the overall branching in the poly(1-hexene*) decreases quite dramatically with temperature (∼100 at 0 °C to ∼60 at 55 °C) since the fraction of 2,1/1° insertions increases rapidly at the expense of 2,1/2° insertions. Surprisingly, the ratio of 2,1/1° to 2,1/2° inverts with temperature, suggesting a more negative ΔS^*

Table 4. Summary of Temperature Effects on 1-Hexene-*2*-^{13}C Polymerization

					% 1,2-ins	% 2,1-ins			
entry	catalyst[a]	temp (°C)	TOF (h^{-1})	Br/1000 C[b]	(1°)[c]	(1°)[d]	(2°)[e]	M_n ($\times 10^{-3}$)[f]	M_w/M_n
1	**1a**	0	907	120/127	67	24	9	83	1.15
2	**1a**	25	1840	119/117	57	33	10	88	1.71
3	**1a**	55	1460	101/107	53	36	11	68	2.08
4	**1b**	0	528	98/103	10	38	52	74	1.19
5	**1b**	25	1410	63/76	14	55	31	81	1.46
6	**1b**	55	680	59/65	14	61	25	40	1.66

[a] Polymerization conditions: 4.0 mM solution of dibromide complex added to mixture of 200 equiv of MAO and 10 vol % 1-hexene* (0.8 M) in toluene. [b] First value from ^{1}H NMR; second value determined from ^{13}C NMR. [c] Determined from sum of integrals for labeled methine C's. For **1a**, a small fraction of 1,2-insertion into secondary bonds occurs (see text). [d] Determined from sum of labeled methylene C's − methylene C's β to a branch (27−28 ppm). [e] Determined from sum of labeled methylene C's β to a branch. [f] All molecular weights from GPC vs polystyrene standards.

Scheme 9

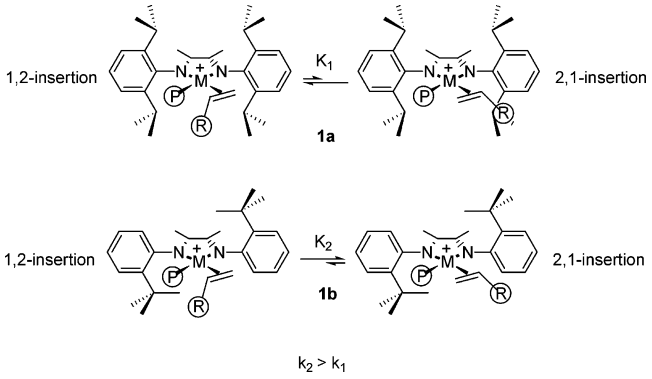

for the 2,1/2 ° process relative to 2,1/1°. The decreased branching in poly(1-hexene) prepared from **1b** relative to **1a** has consequences for the thermal behavior of the polymers. Poly(1-hexene) prepared from **1b** at 25 °C exhibits a T_g at −57 °C and a broad T_m at −17 °C, while the much less branched poly(1-hexene) prepared from **1b** exhibits a T_g of −49 °C and a very broad T_m between ≈0 and 45 °C. Annealing the sample at 24 °C for 16 h resolves this transition into two melt transitions: a broad one centered at 19 °C and a sharp one at 40 °C.

In view of the above results, two mechanistic questions remain. Why does catalyst **1b** exhibit a greater fraction of 2,l-insertions relative to **1a**, and why do 2,1/2° insertions occur only when the secondary alkyl group possesses an α-methyl group (Scheme 8)? If one assumes that the C═C double bond of 1-hexene must be approximately aligned with the Ni−alkyl bond for insertion, then the structures necessary for insertion in each case are shown in Scheme 9. It is reasonable to assume that the steric interactions in these structures reflect the steric interactions in the transition states for insertion. For catalyst **1a** in which both ortho positions are substituted, the alignment necessary for 2,l-insertion always results in interaction of the C-4 substituent with an ortho isopropyl group. In contrast, for catalyst **1b**, 1-hexene can be aligned such that the C-4 substituent interacts with an ortho hydrogen atom. This analysis suggests that K_2 would be greater than K_1, and thus the ratio of 2,l-:1,2-insertion should increase for catalyst **1b** relative to **1a**, as is observed.

Mechanistic studies have shown that, in the case of Ni aryldiimine systems, the catalyst resting state is the alkyl agostic species and that there is substantial chain-walking prior to insertion. Thus, just as in the case of the Pd systems, the alkyl olefin complexes will equilibrate prior to insertion, and the relative ratios of insertion pathways will depend on both the equilibrium ratios of the various olefin complexes as well as their rates of insertion (Curtin−Hammett kinetics). The secondary alkyl 1-hexene complexes which can be formed following a 1,2-insertion are shown below. Structure **10** is favored on steric grounds and, assuming similar insertion barriers for these species, would account for the majority of 2,1/2° insertions occurring through this species with no observable C3 and C2 branches formed via insertions from **8** and **9**.

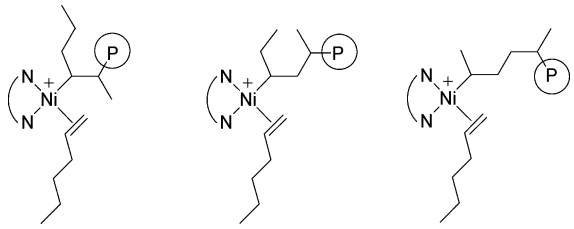

8 **9** **10**

Conclusions

The Pd α-diimine complex, **2**, is a single-component catalyst for the addition polymerization of α-olefins. Linear α-olefins from C_5 to C_{20} were polymerized to give polymers with three major branch lengths: methyl branches, "*a*" branches ($a + 2$ = number of carbons of the α-olefin), and branches equal to or longer than hexyl which could not be differentiated by NMR spectroscopy. The number of branches of each length could be quantified using NMR spectroscopy. The total number of branches and the distribution of branches can be explained by three mechanistic "rules": (1) The olefin can insert into the metal−carbon bond in either a 1,2- or 2,1-manner. (2) Chain-walking of the metal down the hydrocarbon chain occurs via a sequence of β-hydrogen elimination and readdition reactions. The rate of chain-walking is generally greater than the rate of olefin insertion. (3) Insertion occurs only into primary Pd−alkyl bonds.

The fraction of ω,1-enchainment (2,1-insertion followed by chain-walking) ranges from 0.41 to 0.53 and is relatively independent of monomer, indicating that catalyst **2** does not have a significant selectivity for 1,2- vs 2,1-insertion. Following this mechanistic model, certain unique branch-on-branch structures are predicted and have been observed via ^{13}C NMR spectroscopy. For example, the expected 2-methylpentyl branch is observed in poly(1-pentene). A particular set of backbone microstructures is also expected, and these were confirmed to exist in the predicted relative amounts by ^{13}C NMR for polymers of 1-pentene and 1-hexene. The −CH(R)CH_2CH(Me)− structure (R > Me, 42−44 ppm) is unique to these polymers and is not normally found in poly(α-olefins) made with other catalysts. Thermal analysis data also support the microstructures and predictions of these "rules".

For Ni catalysts, to accommodate the results obtained for polymerization of ^{13}C-labeled 1-hexene, the mechanism proposed for the Pd catalysts must be augmented by the addition of steps where insertion occurs at secondary carbons bonds to

give 2,5-enchainment and 1,5-enchainment. Indeed, for one of the poly(1-hexene)s formed from **1b** at 25 °C, 86% of all insertions are 2,1, and nearly half of the 2,1-insertions occur by means of insertion into secondary Ni−alkyl bonds.

Acknowledgment. Many thanks to our colleagues who contributed to this effort. Rich Morrison, Jr., did a large portion of the polymerization work as well as the thermal analysis of the polymers. Molecular weight characterization was provided by Ralph Fuller. Many thanks to Paul Soper, who developed the computational and visual insights into the mechanism of ethylene polymerization. The authors from the University of North Carolina thank the NSF (Grant CHE-0107810) and DuPont for funding. M.B. thanks the Humboldt Foundation for support during a portion of the prolonged preparation of this manuscript.

Supporting Information Available: ^{13}C spectrum of labeled poly(1-hexene) produced using catalyst **1a** and detailed synthetic procedure for preparation of 1-^{13}C-labeled 1-hexene. This material is available free of charge via the Internet at http://pubs.acs.org.

References and Notes

(1) Michael, V. M.; Fink, G. *Angew. Chem., Int. Ed. Engl.* **1985**, *24*, 1001−1003.
(2) Schubbe, R.; Angermund, K.; Fink, G.; Goddard, R. *Macromol. Chem. Phys.* **1995**, *196*, 467−478.
(3) Ketley, A. D.; Braatz, J. A. *Polym. Lett.* **1968**, *6*, 341−343.
(4) Johnson, L. K.; Killian, C. M.; Brookhart, M. *J. Am. Chem. Soc.* **1995**, *117*, 6414−6415.
(5) Johnson, L. K.; Mecking, S.; Brookhart, M. *J. Am. Chem. Soc.* **1996**, *118*, 267−268.
(6) Killian, C. M.; Tempel, D. J.; Johnson, L. K.; Brookhart, M. *J. Am. Chem. Soc.* **1996**, *118*, 11664−11665.
(7) Ittel, S. D.; Johnson, L. K.; Brookhart, M. *Chem. Rev.* **2000**, *100*, 1169−1203.
(8) Mecking, S. *Angew. Chem., Int. Ed.* **2001**, *40*, 534−540.
(9) (a) Britovsek, G. J. P.; Gibson, V. C.; Wass, D. F. *Angew. Chem., Int. Ed.* **1999**, *38*, 428−447. (b) Gibson, V. C.; Spitzmesser, S. K. *Chem. Rev.* **2003**, *103*, 283−315.
(10) Guan, Zhibin; Cotts, P. M.; McCord, E. F.; McLain, S. J. *Science (Washington, D.C.)* **1999**, *283*, 2059−2062.
(11) McCord, E. F.; McLain, S. J.; Nelson, L. T. J.; Arthur, S. D.; Coughlin, E. B.; Ittel, S. D.; Johnson, L. K.; Tempel, D.; Killian, C. M.; Brookhart, M. *Macromolecules* **2001**, *34*, 362−371.
(12) Shultz, L. H.; Tempel, D. J.; Brookhart, M. *J. Am. Chem. Soc.* **2001**, *123*, 11539−11555.
(13) Tempel, D. J.; Brookhart, M. *Organometallics* **1998**, *17*, 2290−2296.
(14) Tempel, D. J.; Johnson, L. K.; Huff, R. L.; White, P. S.; Brookhart, M. *J. Am. Chem. Soc.* **2000**, *122*, 6686−6700.
(15) Killian, C. M.; Tempel, D. J.; Johnson, L. K.; Brookhart, M. *J. Am. Chem. Soc.* **1996**, *118*, 11664−11665.
(16) Pellecchia, C.; Zambelli, A. *Makromol. Chem., Rapid Commun.* **1996**, *17*, 333−338.
(17) Cheriam, A. E.; Rose, J. M.; Lobkovsky, E. B.; Coates, G. W. *J. Am. Chem. Soc.* **2005**, *127*, 13770−13771.
(18) Peruch, F.; Cramail, H.; Deffieux, *Macromolecules* **1999**, *32*, 7977−7983.
(19) Subramanyam, U.; Rajamohanan, P. R.; Sivaram, S. *Polymer* **2004**, *45*, 4063−4076.
(20) Nelson, L. T. J.; McCord, E. F.; Johnson, L. K.; McLain, S. J.; Ittel, S. D. *Polym. Prepr. (Am. Chem. Soc., Div. Polym. Chem.)* **1997**, *38* (1), 133−134.
(21) Tempel, D. J. Thesis, University of North Carolina, Chapel Hill, NC. Avail. UMI, Order No. DA9902525. 1998, 186 pp. from: *Diss. Abstr. Int. B* **1999**, *59*, 4123.
(22) Freche, P.; Grenier-Loustalot, M.; Metras, F. *Makromol. Chem.* **1983**, *184*, 569−83.
(23) Boor, J. *Ziegler−Natta Catalysts and Polymerizations*; Academic Press: New York, 1979.
(24) Kaminsky, W. *Macromol. Chem. Phys.* **1996**, *197*, 3907−3945.
(25) Hungenberg, K.-D.; Kerth, J.; Langhauser, F.; Müller, H.-J.; Müller, P. *Angew. Makromol. Chem.* **1995**, *227*, 159−177.
(26) Brintzinger, H. H.; Fischer, D.; Mülhaupt, R.; Rieger, B.; Waymouth, R. M. *Angew. Chem., Int. Ed. Engl.* **1995**, *34*, 1143−1170.
(27) Zambelli, A.; Locatelli, P.; Provasoli, A.; Ferro, D. R. *Macromolecules* **1980**, *13*, 267.
(28) Ewen, J. A.; Jones, R. L.; Razavi, A.; Ferrara, J. D. *J. Am. Chem. Soc.* **1988**, *110*, 6255−6256.
(29) (a) Miller, J. A.; Irwin, L. J. *J. Am. Chem. Soc.* **2005** *127*, 9972−9973 and references therein. (b) Grisi, E.; Longe, P.; Zambelli, A.; Ewen, J. A. *J. Mol. Catal. A: Chem.* **1999**, *140*, 225−233.
(30) For a general review of propylene polymerizations by metallocenes, see: Resconi, L.; Cavallo, L.; Fait, A.; Piemontesi, F. *Chem. Rev.* **2000**, *100*, 1253−1345.
(31) Nakacho, K. *Idem. Giho* **1991**, *34*, 317−22.
(32) Busico, V.; Cipullo, R.; Borriello, A. *Macromol. Rapid Commun.* **1995**, *16*, 269−274.
(33) Pangborn, A. B.; Giardello, M. A.; Grubbs, R. H.; Rosen, R. K.; Timmers, F. J. *Organometallics* **1996**, *15*, 1518−1520.
(34) (a) Svoboda, M.; tom Dieck, H. *J. Organomet. Chem.* **1980**, *191*, 321−328. (b) tom Dieck, H.; Svoboda, M.; Grieser, T. *Z. Naturforsch.* **1981**, *36B*, 823−832.
(35) (a) Guan, Z.; Cotts, P. M.; McCord, E. F.; McLain, S. J. *Science* **1999**, *283*, 2059−2062. (b) Cotts, P. M.; Guan, Z.; McCord, E. F.; McLain, S. J. *Macromolecules* **2000**, *33*, 6945−6952.
(36) Paul Soper of DuPont used an artificial intelligence algorithm which "learned" to develop probabilities of the required events necessary to describe the quantified features of a large number of inputted structural features and their quantified abundance. These events included insertion or chain-walking at primary, secondary, and tertiary carbon atom sites on the polyethylene backbone. Having determined the relative probabilities of those events, the program would then statistically generate models of the polymer backbone like the one shown herein.
(37) Michalak, A.; Ziegler, T. *J. Am. Chem. Soc.* **2002**, *124*, 7519−7528.
(38) Michalak, A.; Ziegler, T. *Macromolecules* **2003**, *36*, 928−933.
(39) Michalak, A.; Ziegler, T. *Organometallics* **2003**, *22*, 2069−2079.
(40) Gottfried, A. C.; Brookhart, M. *Macromolecules* **2003**, *36*, 3085−3100.

MA061547M